Autonomous Soft Robots Empowered by Chemical Reaction Networks

Giorgio Fusi, Daniele Del Giudice, Oliver Skarsetz, Stefano Di Stefano, and Andreas Walther**

Hydrogel actuators are important for designing stimuli-sensitive soft robots. They generate mechanical motion by exploiting compartmentalized (de) swelling in response to a stimulus. However, classical switching methods, such as manually lowering or increasing the pH, cannot provide more complex autonomous motions. By coupling an autonomously operating pH-flip with programmable lifetimes to a hydrogel system containing pH-responsive and non-responsive compartments, autoonenomous forward and backward motion as well as more complex tasks, such as interlocking of "puzzle pieces" and collection of objects are realized. All operations are initiated by one simple trigger, and the devices operate in a "fire and forget" mode. More complex self-regulatory behavior is obtained by adding chemo-mechano-chemo feedback mechanisms. Due to its simplicity, this method shows great potential for the autonomous operation of soft grippers and metamaterials.

1. Introduction

Traditional robots are typically built from hard materials and use electrical power and computer chips to operate. Even though they can perform a wide range of tasks, they face problems in manipulating delicate objects and lack biocompatibility. Soft robotics seeks to overcome these limitations by designing new classes of devices composed of soft functional materials, controllable through multiple stimuli. This will allow for robotic systems that more closely mimic the natural world, in both form and function.[1] At the core of every soft robotic system are soft actuators capable of changing their shape in response

G. Fusi, O. Skarsetz, A. Walther
Life-Like Materials and Systems
Department of Chemistry
University of Mainz
Duesbergweg 10–14, 55128 Mainz, Germany
E-mail: andreas.walther@uni-mainz.de
D. Del Giudice, S. Di Stefano
Dipartimento di Chimica Università di Roma La Sapienza and ISB-CNR
Sede Secondaria di Roma – Meccanismi di Reazione
P.le A. Moro 5, Roma I-00185, Italy
E-mail: stefano.distefano@uniroma1.it

to an applied signal stimulus,[2] such as stimuli-responsive polymers, or pneumatics and hydraulics.[3] Hydrogels offer an interesting category of soft actuators due to their mechanical similarity to biological tissues, their biocompatibility, and "wet" operation, which are advantageous for the development of bio-compatible and bio-interfaceable soft robots.[4,5] Hydrogel soft actuators operate through changes in swelling in one or more components in relation to an external stimulus, for instance heat, light, solvent, redox state, and pH.[6] This stimuli-responsiveness has been exploited to develop actuating and shape-changing elements, such as linear pullers,[7] helical twisters,[7,8] bilayers, and grabbers.[9–18] Unlike battery-powered and microchip-containing robotics,[19] these soft robotic systems are classically limited in the complexity of autonomous operations because they source their "instructions" and energy for operation from an outside environmental stimulus. However, such environments do not typically undergo complex changes autonomously to pre-encode a behavior.

A pathway toward autonomous soft robotics devices capable of performing more complex tasks is through coupling chemical responsiveness to chemical reaction networks (CRNs) that can provide autonomous trajectories in chemical potential, such as transient or oscillating states with programmable temporal signatures.[20] In the field of oscillators, complex behavior has been achieved by coupling redox-sensitive gels to the Belusov-Zhabotinsky reaction.[21] Although pH oscillators have also been coupled to hydrogel (de)swelling, their autonomy is compromised as they require constant feeding of reactants.[11,12,22] Additionally, hydrogel relaxation was encoded using autocatalytic reaction/diffusion systems.[23] In general, despite the appeal of oscillators, they often require sophisticated chemistry expertise to master the multi-component cocktails, and, more importantly, the frequency and amplitude of the chemical potential can only be poorly controlled as the oscillations otherwise collapse. In contrast, we have recently shown how pH-feedback systems based on CRNs of acid- and base-producing enzymatic and non-enzymatic systems can be precisely controlled in their transient lifetime and pH amplitude.[24,25] We showed that such pH-feedback systems can be coupled to program transient self-assemblies,[26] molecular machines,[27–29] DNA devices,[30] hydrogelation,[24,31,32] or photonics[33] with precise lifetimes. Two aspects are important when aiming to instruct soft robotic devices with autonomous motion by CRNs. Firstly, due to the

**ADVANCED
SCIENCE NEWS**

www.advancedsciencenews.com

**ADVANCED
MATERIALS**

www.advmat.de

inverse relationship between size and response time in hydrogels, there should be excellent control over both the lifetime and the amplitude of the transient state of an autonomous pH-flip. Secondly, the system should be simple to operate.

Here, we introduce the first system-level integration of pH-feedback systems with compartmentalized hydrogel devices to encode autonomous operation of soft actuators. This is achieved by combining a particularly simple one-component acidic pH-flip based on a self-decarboxylating acid with actuators based on pH-responsive and non-pH-responsive hydrogel segments. To demonstrate the unique benefits of this actuator control mechanism, we design "fire and forget" gel devices capable of interlocking with each other and of capturing objects. Finally, we expand upon single-component fuels and couple the acid pH-flip with an antagonistic base-producing urea/urease reaction in a bilayer actuator to demonstrate higher level of chemo-mechano-chemo self-regulation.

2. Results and Discussion

2.1. Coupling a Self-Decarboxylating Acid to a Responsive Hydrogel

Figure 1 displays the basic operational principle of autonomous soft robotic devices using our one component transient pH-flip, based on activated carboxylic acids that display spontaneous pH-dependent decarboxylation in solution.[34] Upon injection of such an activated acid into an aqueous solution, the pH quickly acidifies, and subsequent decarboxylation leads to the formation of a carbanion that quickly scavenges a proton from solution to increase the pH. The decarboxylation rate is dictated by the structure of the carboxylate, and occurs easily in the presence of electron-withdrawing groups in the α position, able to stabilize the resulting carbanion.[35] Although these acids have typically been used as fuels in non-aqueous solvents,[34] as hydrogen bonding with water prevents the crucial decarboxylation,[36] we found that they can also be successfully employed in aqueous systems containing small amounts of co-solvents (e.g., DMSO, Figure S1, Supporting Information). We chose tribromoacetic acid (TBA)[37] as a one-component pH-flip because the resultant transient acidic pH occurs on a suitable timescale (Figure S2, Supporting Information).

The transient pH-flip can be readily controlled by injecting different quantities of TBA into a morpholinopropane sulfonic acid (MOPS) buffer at a starting pH of 7.2. **Figure 2a–d** summarize the effect of injecting 3.5, 4.0, and 5.0 mᴍ fuel into 2.5, 5.0, and 7.0 mᴍ MOPS. Higher fuel/buffer ratios lead to larger and longer pH drops. Figure 2a shows that with a low buffer concentration, any of the three fuel amounts selected will lead to a large pH drop from 7.0 to 2.7–2.5. Lifetimes of the fueled state, given by the time for pH to regain ΔpH/2, show a clear upward trend with more fuel being added, with lifetimes of 40.5, 47.0, and 54.0 h, respectively. At higher buffer concentrations, the effect of fuel concentration is more pronounced. In 5.0 mᴍ MOPS, the pH drops to 3.2, 3.0, and 2.9 with corresponding lifetimes from 14 to 22 to 30 h as fuel concentration increases. In 7.0 mᴍ MOPS, the pH drops to 5.5, 3.8, and 2.8, with lifetimes of 17.5, 5.5, and 15.0 h. Adding insufficient fuel to overcome the buffer (3.5 mᴍ) leads to a small pH drop, and therefore an artificially long lifetime, as the pH quickly re-enters the buffered region. The CO_2 produced in the decarboxylation step is partially scavenged by water, leading to carbonic acid which dissociates to HCO_3^- and H^+, preventing the pH from being restored to its initial value. Apart from CO_2, a stoichiometric amount of bromoform is produced. As a high-boiling organic solvent that does not participate in acid-base equilibria, and given the small amount of fuel required to operate the pH-flips, we expect it to have no effect on the observed pH profile.

In summary, the lifetime of the transient pH drop can be controlled on the timescale of a few hours to multiple days (Figure 2d) by the interplay of the concentrations of fuel and buffer; increasing fuel leads to deeper and longer pH drops, whilst increasing buffer has the opposite effect. Compared to commonly used pH-oscillators,[38,39] or other pH-feedback systems we have previously developed,[24,31] which rely on multi-component reactant systems and require a fine matching between the rates of the involved reactions, this system benefits from a clear simplicity, aiding its application-oriented use.

Next, we combined these pH-flips with a responsive hydrogel to understand how pH couples to shrinking and swelling kinetics on a larger length scale. Our hydrogels are based on aspartic acid N-acrylamide (A^3) crosslinked in a 50:1 molar ratio with poly(ethylene glycol)diacrylate, (PEGDA 6K; MW = 6000 g · mol^{-1}). The hydrogel also includes rhodamine B, responsible for the orange color (see Supporting Information).
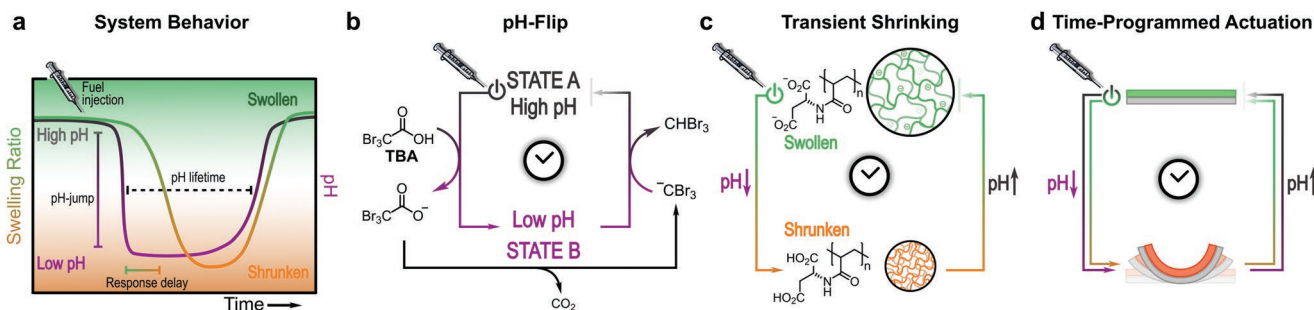
Figure 1. System integration of one-component pH-flips with pH-responsive hydrogels to reach autonomous actuators. a) pH profile (purple line) and actuator response obtained by fueling with tribromoacetic acid. b) Chemistry of the autonomous pH-flip after injecting TBA. c) Transient isotropic hydrogel collapse of poly aspartic acid N-acrylamide hydrogels when coupled to the pH-flip. d) Autonomous and time-programmed anisotropic actuation of a hydrogel bilayer device when coupled to the pH-flip.
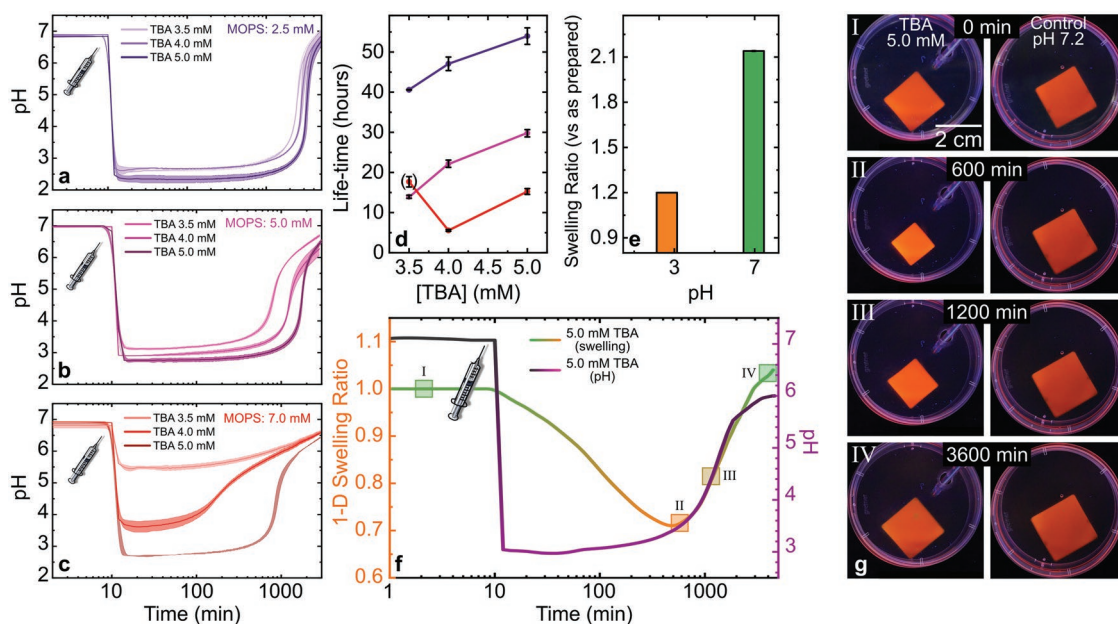
Figure 2. Tuning the pH-flip and coupling it to transient hydrogel deswelling. a–c) pH curves of the TBA CRN at varying concentrations of TBA and MOPS in 70/30 v/v H_2O/DMSO. Shaded contours represent the standard deviation (n = 2 for a, c. n = 3 for b). d) Corresponding lifetimes taken as the time for pH to regain ΔpH/2. The lifetime for 3.5 mM TBA in 7.0 mM MOPS is outside the trend due to the small drop in pH. Error bars indicate the standard deviation (n = 3). e) Equilibrium swelling ratio of the A^3:PEGDA gel. Error bars indicate one standard deviation (< 0.4%; n = 6). f) Transient de-swelling of the gel in (g) alongside the pH experienced by the sample with 5.0 mM TBA fuel. g) Photographs of transiently deswelling gel squares in 5.0 mM MOPS after injection of 5.0 mM TBA. A control is shown for comparison.

The pK_a value of poly(A^3) is at ca. 6.2. This fits into the pH range accessible by the TBA fuel system, and allows to access both swollen and unswollen states in our active gel. The drop in pH below the pK_a value of the gel leads to the progressive protonation of the carboxyl groups, and a shrinking of the gel network through a combination of lower electrostatic repulsion between chain segments and less favorable gel-solvent interactions. Indeed, the equilibrium swelling ratio, normalized to the specimen dimensions during synthesis in a mold, shows a decrease in 1D swelling ratio from 2.2 at pH 7 to 1.2 at pH 3, hence a collapse to 45% of the original volume (Figures 2e; Figure S3, Supporting Information). To demonstrate coupling between pH-flip and gels, we fueled gel squares of 2.0 × 2.0 × 0.5 cm in 5 mM MOPS buffer at pH 7.2 with 5.0 mM TBA (Figures 2f,g). The gel contraction reaches 70% of the original dimensions when fueled. Due to the slow mass transport of water out of the gel, a significant lag time between reaching the lowest pH point and the maximum deswelling occurs, which underscores the importance of being able to tune the transient pH state over long periods.

2.2. Exploiting Transient Deswelling for Actuating Elements

In order to exploit this transient deswelling for autonomous motion, we paired the A^3-gel with a non-responsive gel made of 2-acrylamido-2-methylpropane sulfonic acid (AMPS; crosslinked in a 50:1 molar ratio with PEGDA 6K) into bilayer devices. This hydrogel contains the fluresceine dye responsible for the faint green color (see Supporting Information). Poly(AMPS) is a strong polyelectrolyte with a pK_a of 1.5,[40] and

was selected as a passive layer due to its equilibrium swelling being close to that of the poly(A^3) gel, while not displaying pH-responsiveness in the pH range of this study. The mechanical properties of both the active and passive gels are shown in Figure S4 (Supporting Information). The bilayers are manufactured by partially photocuring each layer separately in a 30 × 2 × 2 mm PTFE mold, and overlaying them for a final photocuring step, ensuring robust interfacial adhesion (**Figure 3**a). The bilayers are then soaked in 5.0 mM MOPS pH 7.2 to reach their final state, which is slightly bent due to smaller swelling of poly(AMPS). The bilayers are then cut shorter to 58 mm and mounted on a support before being attached to a container for fueling experiments.

To demonstrate the control over the magnitude and duration of the actuation, we fueled bilayers with 3.0, 5.0, and 7.0 mM TBA in 5.0 mM MOPS (Figures 3b–d, Movie S1, Supporting Information). When fueled with 3.0 mM TBA, a pH drop from 7 to 3.5 with a duration of 250 mins is observed. The active layer does not have enough time to equilibrate before the pH returns to its original value, leading to only minimal bending. This indicates the actuators require a threshold amount of fuel and transient lifetime to display motion. This threshold quantity is a function of the total size of the hydrogel device, as in a rod-like hydrogel, (de)swelling time scales with the radius squared.[41] In contrast, bilayers fueled with 5.0 and 7.0 mM TBA display a clear bending response, with more fuel leading to a longer and larger change in bending angle. Fueling with 5.0 mM TBA leads to a pH drop from ca. 7.0 to 3.0, and to a transient peak bending of 150°. The bilayer fueled with 7.0 mM TBA experiences a pH drop from 7.0 to 2.0, and correspondingly a longer contraction of the active layer and a peak bending
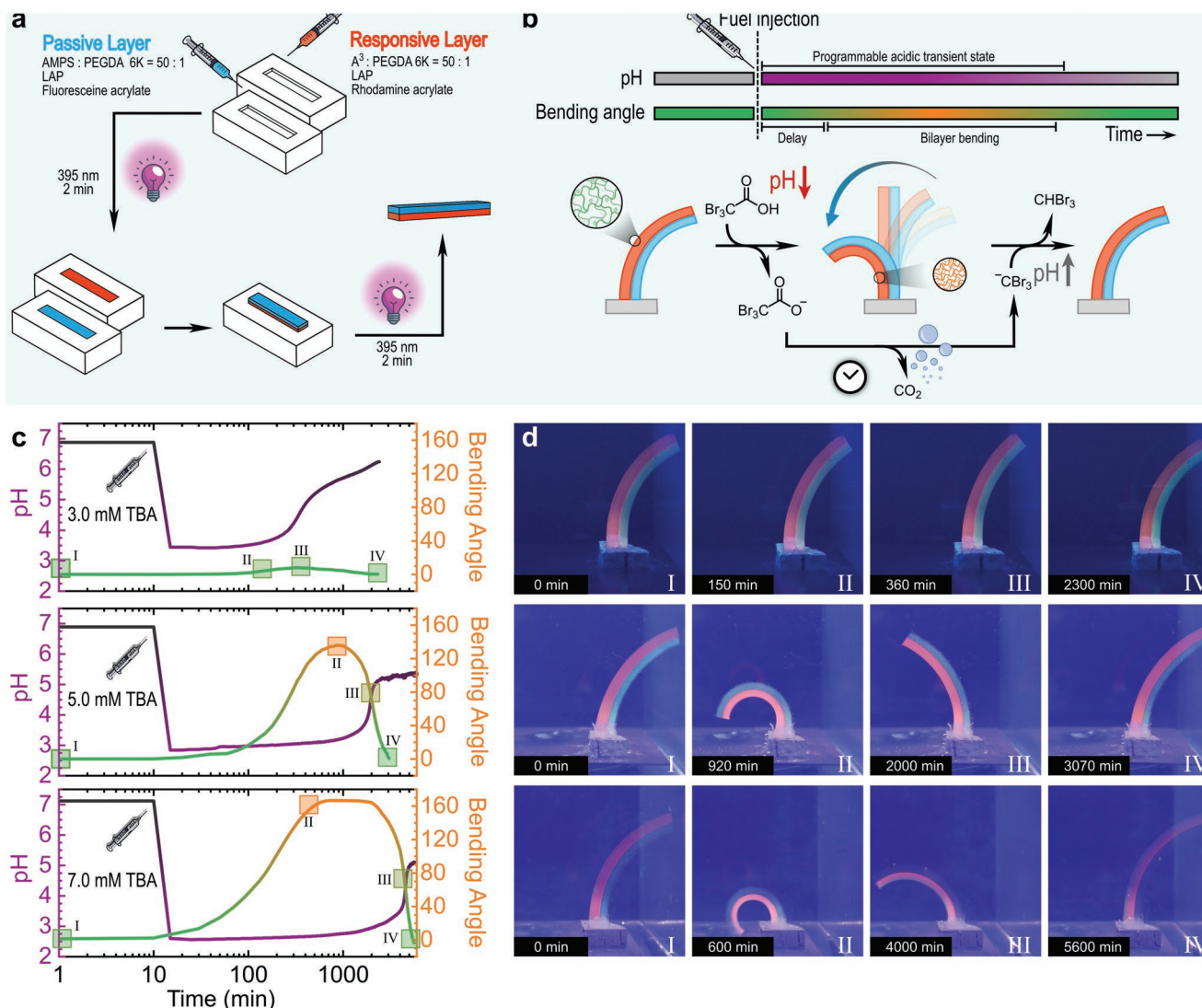
Figure 3. Autonomous bilayer actuators controlled by transient pH flips. a) Fabrication of the bilayer devices by mold-casting and photocuring. Mold dimensions are $30 \times 2 \times 2$ mm. Swollen active layer is $62 \times 4 \times 4$ mm. AMPS layer shows lower swelling, leading to a curved conformation. b) Schematic representation of the effect of the TBA CRN on the bilayer devices. c) Effect of differing fuel concentrations on the magnitude and duration of the pH drop in 5.0 mM MOPS, and the corresponding change in bilayer angle. d) Photographs of the corresponding bilayers at select time intervals. Related videos are also available in the Supporting Information.
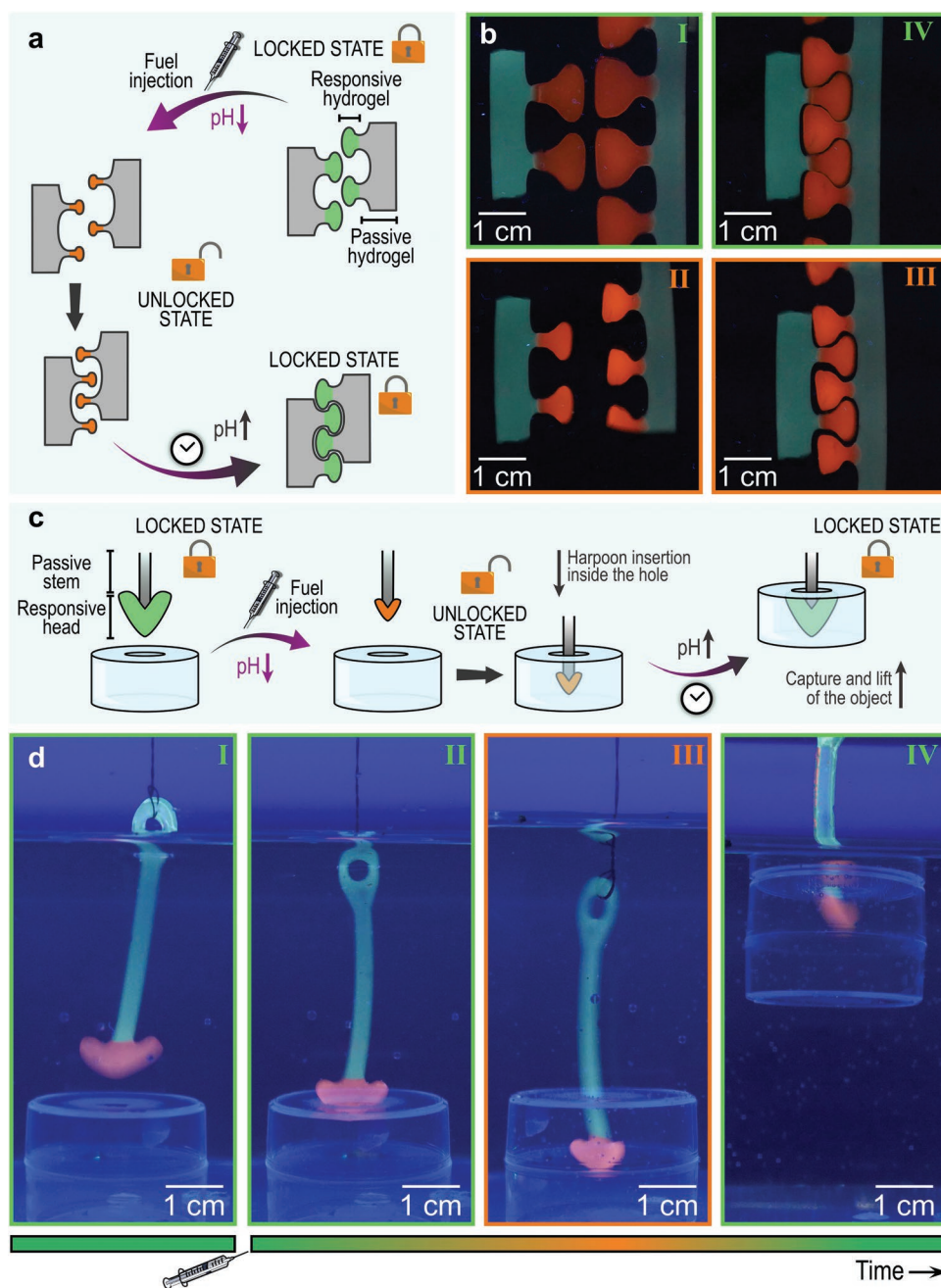
angle change of 160°, demonstrating fuel-dependent actuator response.

2.3. Temporal Pre-Programming for Fire and Forget Devices

Next, we demonstrate the advantages of temporal pre-programming of these hydrogel actuators, as compared to classical responsive devices. These devices can operate in a "fire and forget" mode, where fueling leads to a predetermined actuation sequence. This can be interesting for systems, where delivering successive external stimuli is not possible. For instance, we prepared complementary "puzzle piece" gels with responsive A^3 and unresponsive AMPS segments (**Figure** 4b; panel I). These complementary puzzle pieces are capable of interlocking, but cannot be slid one into the other due to the width of the heads

being larger than the gap between them. On fueling with a critical amount of TBA, the orange active gel contracts. Since the gap is now big enough, the two puzzle pieces can be pushed together, and the active components interdigitate (Figure 4b; panels II and III). As the acid fuel decarboxylates and the pH rises, the gels reswell, and are eventually fully interlocked and cannot be pulled apart (Figure 4b; panel IV). This operation is conditional on the amount of fuel in the system, as we have learned (Figure 3) that gel contraction occurs in a delayed fashion with respect to the pH-flip curve.

Secondly, fuel-mediated interlocking can also be exploited with just one active gel, as displayed by the gel harpoon (Figure 4c). The harpoon can be used to capture and move objects with an opening smaller than the unfueled head (Figure 4c; panel I). On fueling, the head, with a width of 14 mm, contracts and passes through a 10 mm hole drilled into

**ADVANCED
SCIENCE NEWS**

www.advancedsciencenews.com

**ADVANCED
MATERIALS**

www.advmat.de

Figure 4. Autonomous interlocking of fueled gel devices and grabbing of objects with small orifices. a) Scheme describing the operation of the smart "puzzle piece" gels. b) Interdigitating complementary "puzzle piece" interfaces. The orange parts are composed of pH-responsive gel. I. Unfueled and incapable of interdigitating. II. Fueled and contracted heads. III. Interdigitated due to reduced size. IV. Reswollen to initial size. Carried out in 5.0 mm MOPS with 5.0 mm TBA fuel. c) Scheme describing the operation of the "fire and forget" harpoon device for autonomous grabbing of objects with small orifices. d) Harpoon device. From left to right: harpoon being lowered over opening, harpoon head resting on opening and unable to spear object, once fueled, head contracts and passes through opening, harpoon being lifted and taking object with it after re-expansion of head. Carried out in 5.0 mm MOPS with 5.0 mm TBA fuel.

a plastic cylinder (Figure 4c; panel II and III). Once the fueling cycle ends and the gel reswells, the harpoon can be lifted to take the captured load with it (Figure 4c; panel IV). In contrast to classical responsive devices that would require re-addition of chemicals, these devices are "fire-and-forget" and perform their autonomous operation without further user intervention, which allows for more flexible application scenarios and more complex interlocking of spaces that are poorly accessible from outside (e.g., the interior of the device captured by the harpoon).

2.4. Coupling to Urea / Urease Reaction for Chemomechanical Feedback

One of the key aspects of such autonomous devices enabled by CRNs is the possibility to add a higher-level autonomous control mechanism, by for instance embedding further antagonistic reaction modules at specific locations within the device. This multifunctionality enables chemomechanical feedback and self-regulation downstream of the initial fueling event. To demonstrate this, the TBA cycle is coupled to the urea/urease enzymatic reaction.[25,32] Urease is useful to couple to in this context, as it converts urea to ammonia and carbon dioxide, therefore leading to a rise in pH. As a device, we incorporated a cylindrical patch (h = 4 mm, r = 3.5 mm) containing 10 mg mL^{-1} urease atop an A^3/AMPS bilayer like those shown in Figure 3. This bilayer is then placed in a container containing a 100 mM urea solution in 5.0 mM MOPS, with an additional dodecane phase on top. Before fueling, the bilayer points out of the bottom aqueous phase and the urease-containing gel patch is located inside the dodecane top layer and cannot contact the urea. This avoids the enzymatic production of ammonia. Once fueled with 5.0 mM TBA, the bilayer bends, and brings the urease-containing patch into contact with the aqueous urea-containing solution. This initiates chemo-mechanical feedback by enzymatic conversion of urea into ammonia. This is in fact visible by the increased fluorescein fluorescence as the pH increases[42] in the pas-

sive gel next to the urease-containing block (Figures 5a,b). To quantify the effect of the added chemo-mechanical control mechanism, Figures 5c,d compare the pH profiles and the maximum bending angle of a system with a urease patch with an identical system without urease as a control. The maximum bending angles achieved are similar in both systems. However, the chemo-mechanical feedback begins raising the pH more quickly than the decarboxylation of the TBA could do alone, and hence significantly shortens the lifetime of the pH drop to less than 50%, from 16.5 h to 6 h (**Figure 5**c). The added weight of the urease gel on top of the bilayer leads to some out of plane bending in the experiments, making the gel appear shorter in the final images. To confirm the effect of chemo-mechanical feedback, meaning the necessity of the urease patch to dive into the aqueous bottom layer and exclude urea diffusion though the bilayer to the urease-containing patch in the dodecane upper phase, we placed a non-bending homogenous AMPS post with a urease gel patch on top in the same two-phase system. Figure 5c shows there is no change in aqueous phase pH over the course of the experiment. This confirms that no enzyme leakage occurs, and that the quicker pH feedback and chemo-mechanical return of the bilayer is indeed conditional on the urease patch diving into the fuel solution. Employing chemo-mechano-chemo feedback systems allows for higher self-regulation capacity, as the device can now sense externally present chemicals that are locally transduced into effectors.
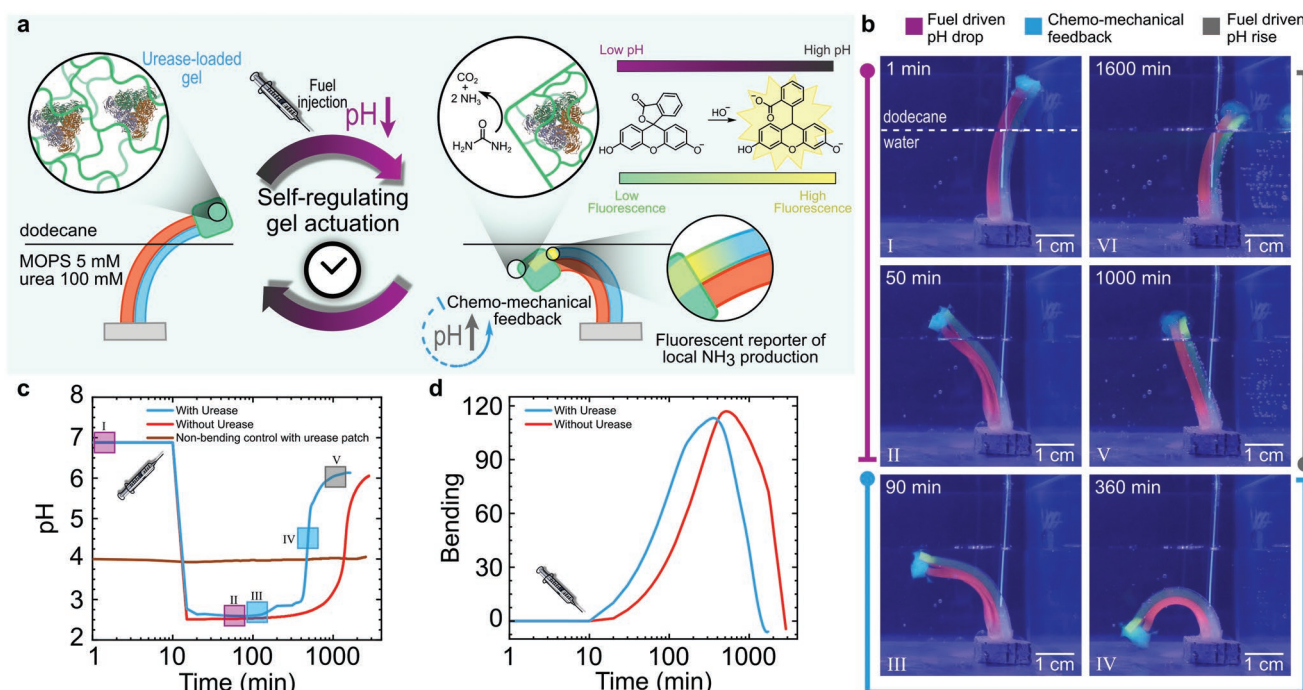
Figure 5. Chemo-mechanical feedback regulation of pH using the urea/urease enzymatic reaction. a) Design of the urease-containing gel. A highly crosslinked gel containing urease is attached to the top of an A^3/AMPS bilayer. When the bilayer bends below the dodecane-water interface, the catalytic conversion of urea to ammonia begins. This can be visualized through the increased fluorescence (the apparent color changes from faint green to bright yellow) of the AMPS gel in proximity to the urease loaded gel. b) Photographs showing the bilayer during a representative experiment. c) pH profiles of the water phase in the experiment pictured in (b), a representative experiment without the urease-containing gel (both in 5.0 mM MOPS with 5.0 mM TBA fuel), and a control of an inert post holding the urease gel in the dodecane phase, with the water phase being 3.0 mM citrate. d) Bending profiles of the bilayers mentioned in (c).

**ADVANCED
SCIENCE NEWS**

www.advancedsciencenews.com

**ADVANCED
MATERIALS**

www.advmat.de

3. Conclusion

In summary, this study has introduced a new method of autonomous control for soft robotic actuators by integrating autonomous chemical controllers in the form of transient pH-flips with pH-responsive hydrogels. In contrast to the complex cocktails often needed for other chemical controllers for autonomous systems,[43] specifically, CRNs suitable for polymers,[21,23,44] our system is particularly simple to operate due to the use of a one-component pH-flip. Indeed, it can be conveniently applied by a simple injection and allows a wide control over the lifetime and amplitude of the pH-flip. Compared to well-known clock reactions[38,39] or our earlier pH feedback systems,[24,31] this system can be operated with a reduced number of components and in a batch setting. Furthermore, the duration and amplitude of the pH-flip can be easily controlled by altering the amount of TBA fuel or buffer, rather than requiring fine-tuning of multiple component reactions. In addition to the control over bending angle of a bilayer as a function of the lifetime, we demonstrated applications where autonomous operation might be useful, e.g., for the autonomous interlocking of interfaces and for grabbing objects with small orifices, where other stimuli would be difficult to apply. We also introduced how chemo-mechanical feedback can be included to achieve autonomous self-regulation of the device. On a fundamental level, this combination of responsive elements with advanced chemical control is vital for the transition from classical switchable materials to more life-like materials systems capable of autonomous, adaptive, and self-regulated behavior.[45]

Given that our simple one-component method to achieve autonomous control is compatible "out of the box" with pH responsive soft robot devices, we expect that this will "democratize" autonomous chemical controllers for material applications. Further research to find more environmentally benign self-decarboxylating acids will help to broaden the possible applications of this method. We further believe it is likely to be of great interest in systems where the delivery of successive fuels, complex fuel mixtures or physical stimuli is impractical, such as non-electronic and self-contained devices designed for autonomous operation, for example in microfluidic systems. The devices here shown, capable of "fire and forget" operation, could be used in smart implants, a growing interest in the biomedical field. Devices including chemomechanical feedback capabilities could lead to possible applications where fine control and feedback are necessary, such as prosthetics.

Supporting Information

Supporting Information is available from the Wiley Online Library or from the author.

Conflict of Interest

The authors declare no conflict of interest.

Data Availability Statement

The data that support the findings of this study are available from the corresponding author upon reasonable request.

[1] G. M. Whitesides, *Angew. Chem. Int. Ed.* **2018**, *57*, 4258.
[2] N. El-Atab, R. B. Mishra, F. Al-Modaf, L. Joharji, A. A. Alsharif, H. Alamoudi, M. Diaz, N. Qaiser, M. M. Hussain, *Adv. Intell. Syst.* **2020**, *2*, 2000128.
[3] J. Wang, D. Gao, P. S. Lee, *Adv. Mater.* **2021**, *33*, 2003088.
[4] M. Cianchetti, C. Laschi, A. Menciassi, P. Dario, *Nat. Rev. Mater.* **2018**, *3*, 143.
[5] H. Banerjee, M. Suhail, H. Ren, *Biomimetics* **2018**, *3*, 15.
[6] M. Ding, L. Jing, H. Yang, C. E. Machnicki, X. Fu, K. Li, I. Y. Wong, P.-Y. Chen, *Mater. Today Adv.* **2020**, *8*, 100088.
[7] H. Arslan, A. Nojoomi, J. Jeon, K. Yum, *Adv. Sci.* **2019**, *6*, 1800703.
[8] R. M. Erb, J. S. Sander, R. Grisch, A. R. Studart, *Nat. Commun.* **2013**, *4*, 1712.
[9] P. Techawanitchai, M. Ebara, N. Idota, T.-A. Asoh, A. Kikuchi, T. Aoyagi, *Soft Matter* **2012**, *8*, 2844.
[10] J.-Y. Wang, F. Jin, X.-Z. Dong, J. Liu, M.-L. Zheng, *Adv. Mater.* **2022**, *7*, 2200276.
[11] C. Yang, F. Su, Y. Liang, W. Xu, S. Li, E. Liang, G. Wang, N. Zhou, Q. Wan, X. Ma, *Soft Matter* **2020**, *16*, 2928.
[12] C. Yang, F. Su, Y. Xu, Y. Ma, L. Tang, N. Zhou, E. Liang, G. Wang, J. Tang, *ACS Macro Lett.* **2022**, *11*, 347.
[13] X. He, Y. Sun, J. Wu, Y. Wang, F. Chen, P. Fan, M. Zhong, S. Xiao, D. Zhang, J. Yang, J. Zheng, *J. Mater. Chem. C* **2019**, *7*, 4970.
[14] X. Kong, Y. Li, W. Xu, H. Liang, Z. Xue, Y. Niu, M. Pang, C. Ren, *Macromol. Rapid Commun.* **2021**, *42*, 2100416.
[15] J. Liu, W. Xu, Z. Kuang, P. Dong, Y. Yao, H. Wu, A. Liu, F. Ye, *J. Mater. Chem. C* **2020**, *8*, 12092.
[16] X. Wang, H. Huang, H. Liu, F. Rehfeldt, X. Wang, K. Zhang, *Macromol. Chem. Phys.* **2019**, *220*, 1800562.
[17] Z. Jiang, M. L. Tan, M. Taheri, Q. Yan, T. Tsuzuki, M. G. Gardiner, B. Diggle, L. A. Connal, *Angew. Chem. Int. Ed.* **2020**, *59*, 7049.
[18] L. Yang, T. Zhang, W. Sun, *J. Appl. Polym. Sci.* **2020**, *137*, 49375.
[19] S. I. Rich, R. J. Wood, C. Majidi, *Nat. Electron.* **2018**, *1*, 102.
[20] R. Merindol, A. Walther, *Chem. Soc. Rev.* **2017**, *46*, 5588.
[21] R. Yoshida, *Adv. Mater.* **2010**, *22*, 3463.
[22] T. Mikanohara, S. Maeda, Y. Hara, S. Hashimoto, *Adv. Robot.* **2014**, *28*, 457.

2209870 (7 of 8)

**ADVANCED
SCIENCE NEWS**

www.advancedsciencenews.com

**ADVANCED
MATERIALS**

www.advmat.de

[23] A. Paikar, A. I. Novichkov, A. I. Hanopolskyi, V. A. Smaliak, X. Sui, N. Kampf, E. V. Skorb, S. N. Semenov, *Adv. Mater.* **2022**, *34*, 2106816.

[24] T. Heuser, E. Weyandt, A. Walther, *Angew. Chem. Int. Ed.* **2015**, *54*, 13258.

[25] X. Fan, A. Walther, *Angew. Chem. Int. Ed.* **2021**, *60*, 3619.

[26] C. Sharma, A. Walther, *Angew. Chem. Int. Ed.* **2022**, *61*, 202201573.

[27] J. A. Berrocal, C. Biagini, L. Mandolini, S. Di Stefano, *Angew. Chem. Int. Ed.* **2016**, *55*, 6997.

[28] C. Biagini, S. Albano, R. Caruso, L. Mandolini, J. A. Berrocal, S. Di Stefano, *Chem. Sci.* **2018**, *9*, 181.

[29] D. Del Giudice, E. Spatola, R. Cacciapaglia, A. Casnati, L. Baldini, G. Ercolani, S. Di Stefano, *Chem.one Eur. J.* **2020**, *26*, 14954.

[30] D. Mariottini, D. Del Giudice, G. Ercolani, S. Di Stefano, F. Ricci, *Chem. Sci.* **2021**, *12*, 11735.

[31] L. Heinen, T. Heuser, A. Steinschulte, A. Walther, *Nano Lett.* **2017**, *17*, 4989.

[32] I. Maity, C. Sharma, F. Lossada, A. Walther, *Angew. Chem. Int. Ed.* **2021**, *60*, 22537.

[33] T. Heuser, R. Merindol, S. Loescher, A. Klaus, A. Walther, *Adv. Mater.* **2017**, *29*, 1606842.

[34] C. Biagini, S. Di Stefano, *Angew. Chem. Int. Ed.* **2020**, *59*, 8344.

[35] D. J. B. Lydia, L. Lifongo, P. Brimblecombe, *Int. J. Phys. Sci.* **1992**, *5*, 738.

[36] D. D. Giudice, E. Spatola, M. Valentini, C. Bombelli, G. Ercolani, S. Di Stefano, *Chem. Sci.* **2021**, *12*, 7460.

[37] V. W. L. Gunawardana, T. J. Finnegan, C. E. Ward, C. E. Moore, J. D. Badjic, *Angew. Chem. Int. Ed.* **2022**, *61*, 202207418.

[38] G. Rabai, I. Hanazaki, *J. Phys. Chem.* **1996**, *100*, 10615.

[39] P. Warneck, *J. Chem. Educ.* **1989**, *66*, 334.

[40] H. Valle, J. Sánchez, B. L. Rivas, *J. Appl. Polym. Sci.* **2015**, *132*, 41272.

[41] Y. Li, T. Tanaka, *J. Chem. Phys.* **1990**, *92*, 1365.

[42] H. Che, B. C. Buddingh, J. C. M. van Hest, *Angew. Chem. Int. Ed.* **2017**, *56*, 12581.

[43] N. Singh, G. J. M. Formon, S. De Piccoli, T. M. Hermans, *Adv. Mater.* **2020**, *32*, 1906834.

[44] I. Piergentili, P. R. Bouwmans, L. Reinalda, R. W. Lewis, B. Klemm, H. Liu, R. M. de Kruijff, A. G. Denkova, R. Eelkema, *Polym. Chem.* **2022**, *13*, 2383.

[45] A. Walther, *Adv. Mater.* **2020**, *32*, 1905111.